

Supplementary Information for

PD-L1-expressing cancer-associated fibroblasts induce tumor immunosuppression and contribute to poor clinical outcome in esophageal cancer

Authors: Kento Kawasaki¹, Kazuhiro Noma¹, Takuya Kato¹, Toshiaki Ohara^{1,2}, Shunsuke Tanabe¹, Yasushige Takeda¹, Hijiri Matsumoto¹, Seitaro Nishimura¹, Tomoyoshi Kunitomo¹, Masaaki Akai¹, Teruki Kobayashi¹, Noriyuki Nishiwaki¹, Hajime Kashima¹, Naoaki Maeda¹, Satoru Kikuchi¹, Hiroshi Tazawa^{1,3}, Yasuhiro Shirakawa^{1,4}, and Toshiyoshi Fujiwara¹

Affiliations:

¹ Department of Gastroenterological Surgery, Okayama University Graduate School of Medicine, Dentistry and Pharmaceutical Sciences, Okayama, Japan.

² Department of Pathology & Experimental Medicine, Okayama University Graduate School of Medicine, Dentistry and Pharmaceutical Sciences, Okayama, Japan.

³ Center for Gene and Cell Therapy, Okayama University Hospital, Okayama, Japan.

⁴ Department of Surgery, Hiroshima City Hiroshima Citizens Hospital

*Corresponding author. Kazuhiro Noma, Department of Gastroenterological Surgery, Okayama University Graduate School of Medicine, Dentistry, and Pharmaceutical Sciences, 2-5-1 Shikata-cho, Kita-ku, Okayama 700-8558, Japan Phone: +81-86-235-7255; Fax: +81-86-221-8775; E-mail: knoma@md.okayama-u.ac.jp

List of Supplementary Information

Supplementary Figure S1. Representative pictures of PD-L1 expression in the stromal area

Supplementary Figure S2. Comparison of immune cells between PD-L1[±] cancer cell groups

Supplementary Figure S3. Survival curves for the variance of PD-L1 expression

Supplementary Figure S4. Gating strategy and evaluation of PD-L1 expression

Supplementary Figure S5. Dot plots of co-culture models using Cytotell UltraGreen

Supplementary Figure S6. PD-L1 expression in fibroblasts and OE33 cells stimulated by the cancer-conditioned medium of esophageal adenocarcinoma cell lines

Supplementary Figure S7. PD-L1 expression in FEF3 stimulated by TGF- β or conditioned medium of esophageal squamous cell carcinoma cells.

Supplementary Figure S8. Gating strategy and evaluation for PD-L1 in cancer cells and CAFs in vivo models

Supplementary Figure S9. Representative pictures of immunohistochemical staining for CD8, FoxP3, and α SMA in tumor tissues

Supplementary Figure S10. Digoxigenin-labeled anti-PD-L1 antibody administration for murine subcutaneous tumors

Supplementary Figure S11. Representative pictures of immunohistochemical staining for CD8 and FoxP3 in MC38 and SCCVII tumors without MEF

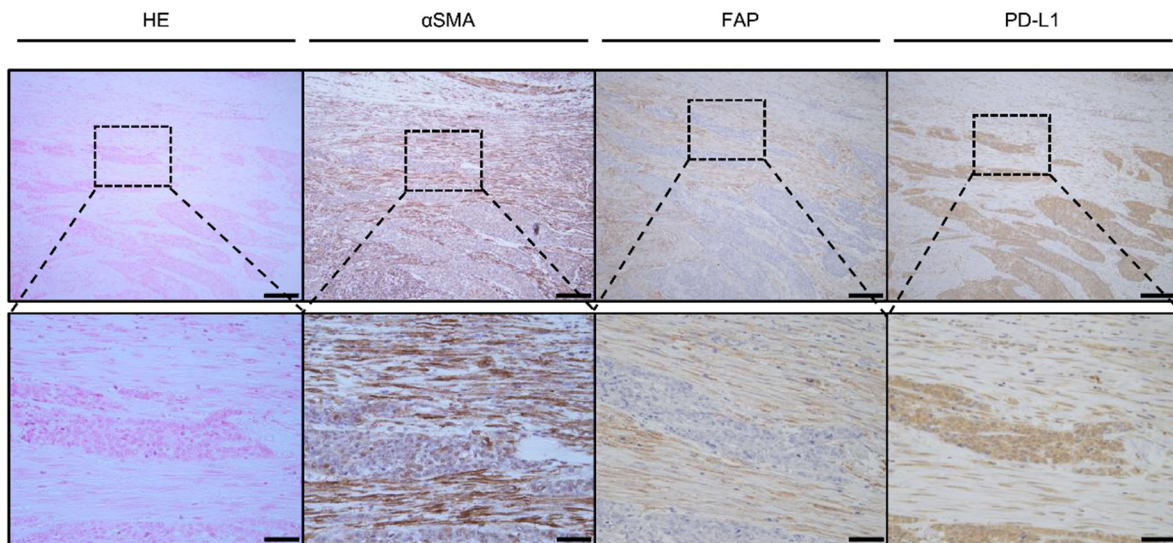
Supplementary Table S1. Clinicopathological features for PD-L1 in cancer cells

Supplementary Table S2. Univariate and multivariate analysis for overall survival

Supplementary Table S3. Univariate and multivariate analysis for relapse-free survival

Supplementary Table S4. Univariate and multivariate analysis for PD-L1 expression in cancer cells

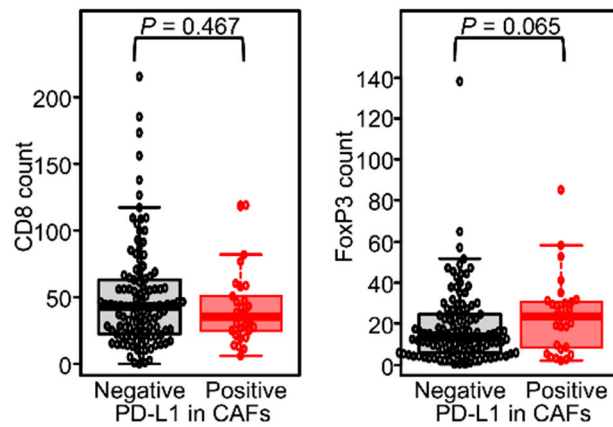
Supplementary Figure S1



Supplementary Figure S1. Representative pictures of PD-L1 expression in the stromal area

Representative images of hematoxylin and eosin staining, α -SMA, FAP, and PD-L1 immunostaining. Scale bars = 100 μ m. The lower figures are enlarged images. Scale bars = 50 μ m.

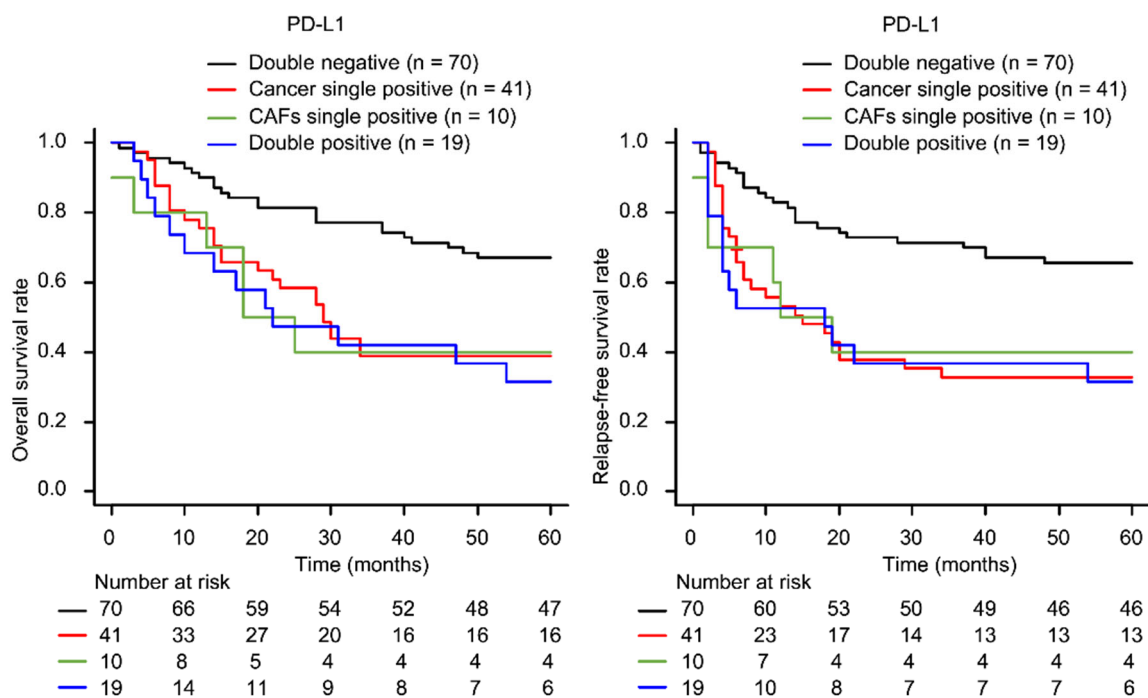
Supplementary Figure S2



Supplementary Figure S2. Comparison of immune cells between PD-L1^{+/-} cancer cell groups

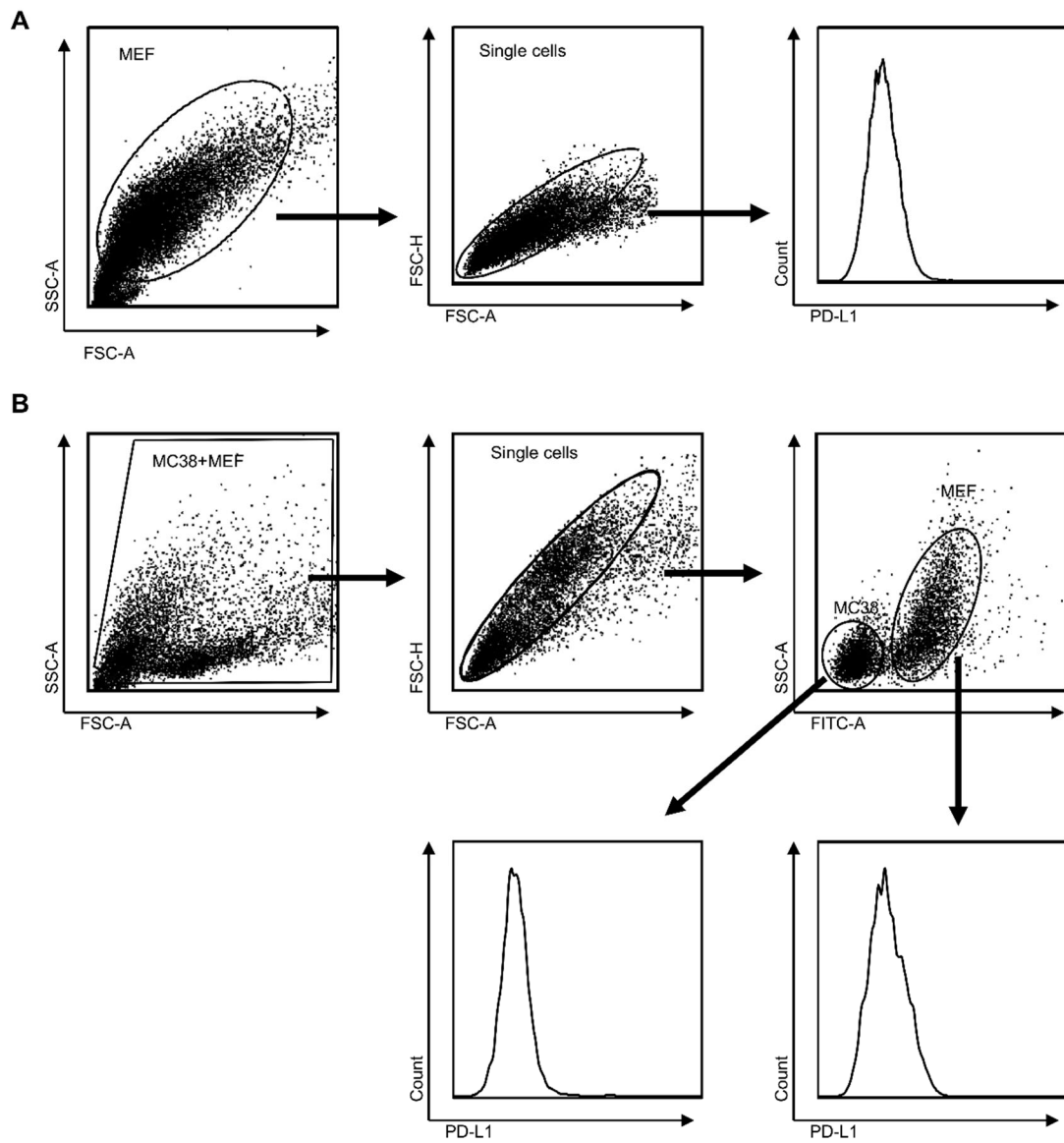
Comparison of CD8⁺ and FoxP3⁺ cells between PD-L1^{+/-} CAFs groups. Mann–Whitney U test.

Supplementary Figure S3

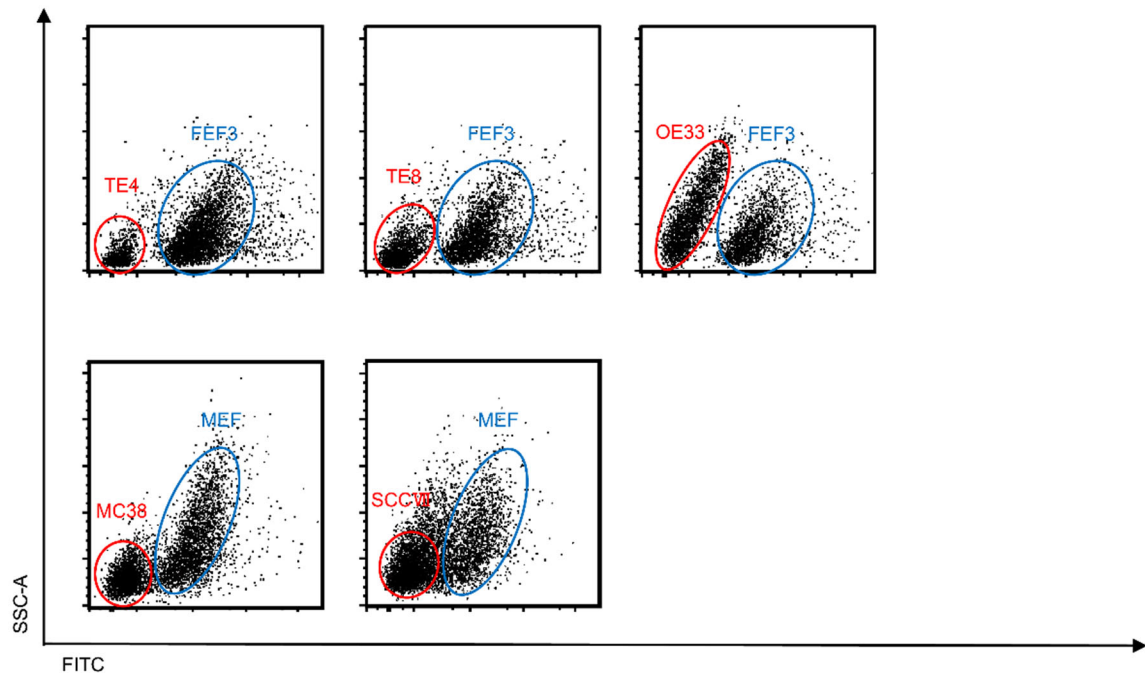


Supplementary Figure S3. Survival curves for the variance of PD-L1 expression

Survival curve according to the variance of PD-L1 expression analyzed using the Kaplan–Meier method (n = 140).

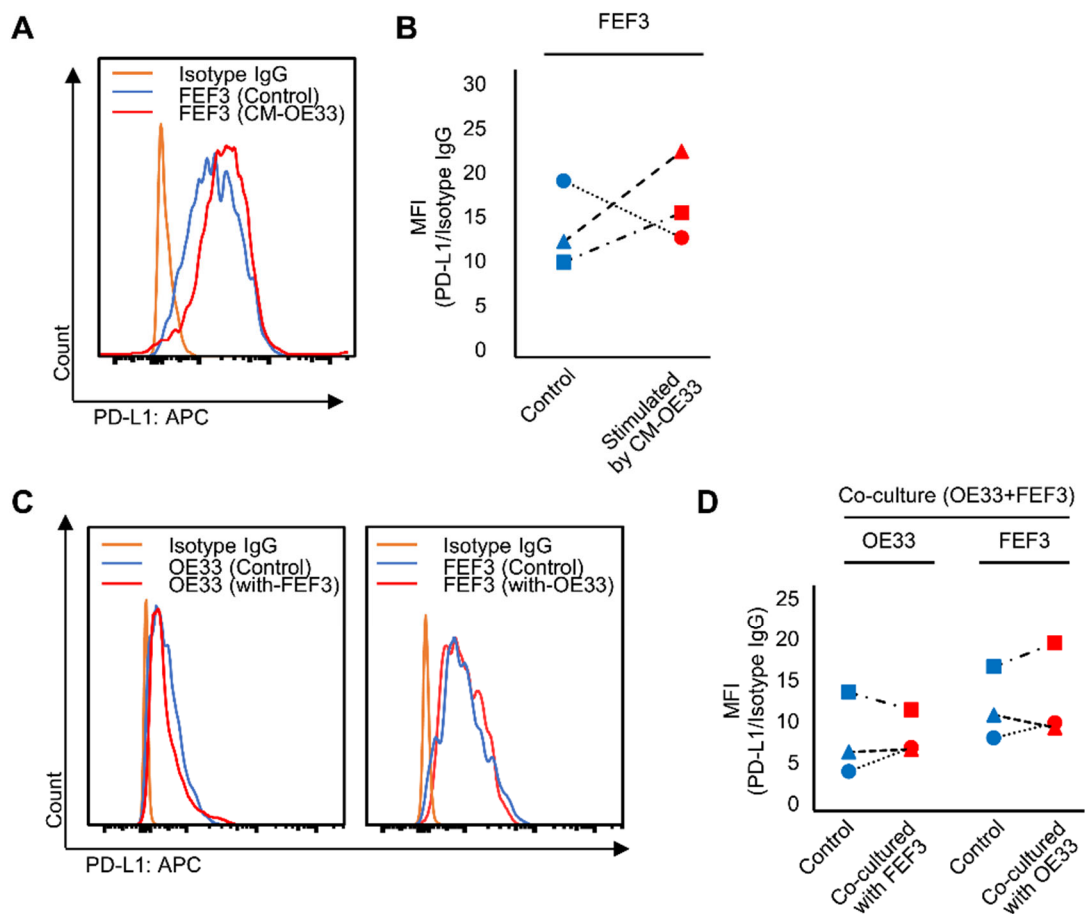
Supplementary Figure S4**Supplementary Figure S4. Gating strategy and evaluation of PD-L1 expression**

Gating strategy and representative histogram via flow cytometry of (A) fibroblasts activated by conditioned media and (B) cancer cells and fibroblasts activated in co-culture models.

Supplementary Figure S5**Supplementary Figure 5. Dot plots of co-culture models using Cytotell UltraGreen**

Representative dot plots by flow cytometric analysis. Fibroblasts were detected using FITC and distinguished from cancer cells by pre-staining with ultra-green.

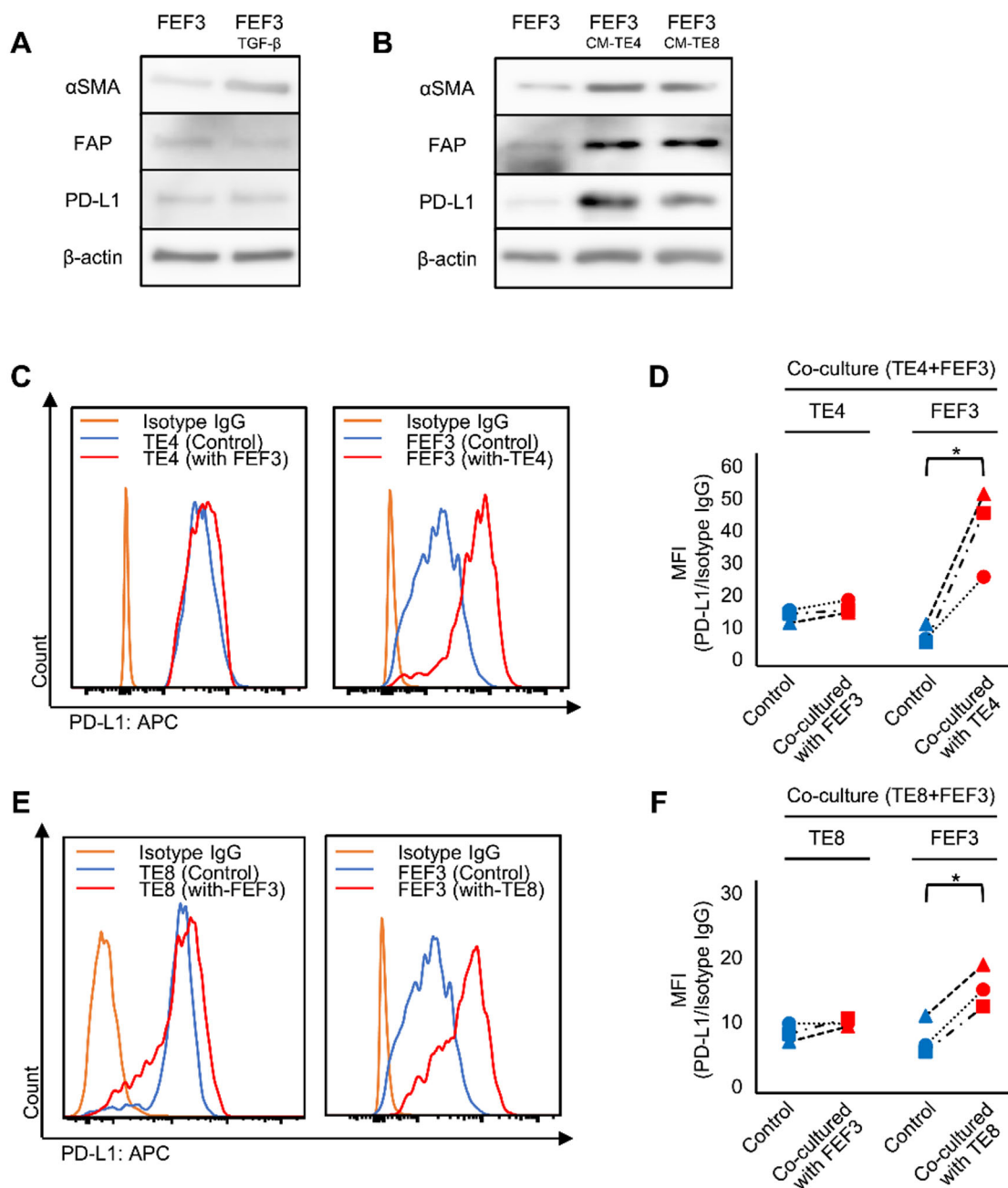
Supplementary Figure S6



Supplementary Figure S6. PD-L1 expression in fibroblasts and OE33 cells stimulated by the cancer-conditioned medium of esophageal adenocarcinoma cell lines

(A, B) Flow cytometry analysis of cell surface PD-L1 expression in fibroblasts with or without activation by conditioned medium from OE33 cells. (A) Histogram and (B) comparison of PD-L1 expression. (C, D) Flow cytometry analysis of cell surface PD-L1 expression in OE33 cells and FEF3 in a co-culture model. (C) Histogram and (D) comparison of PD-L1 expression. $n = 3$, comparative analysis of mean fluorescence intensities using paired t -test.

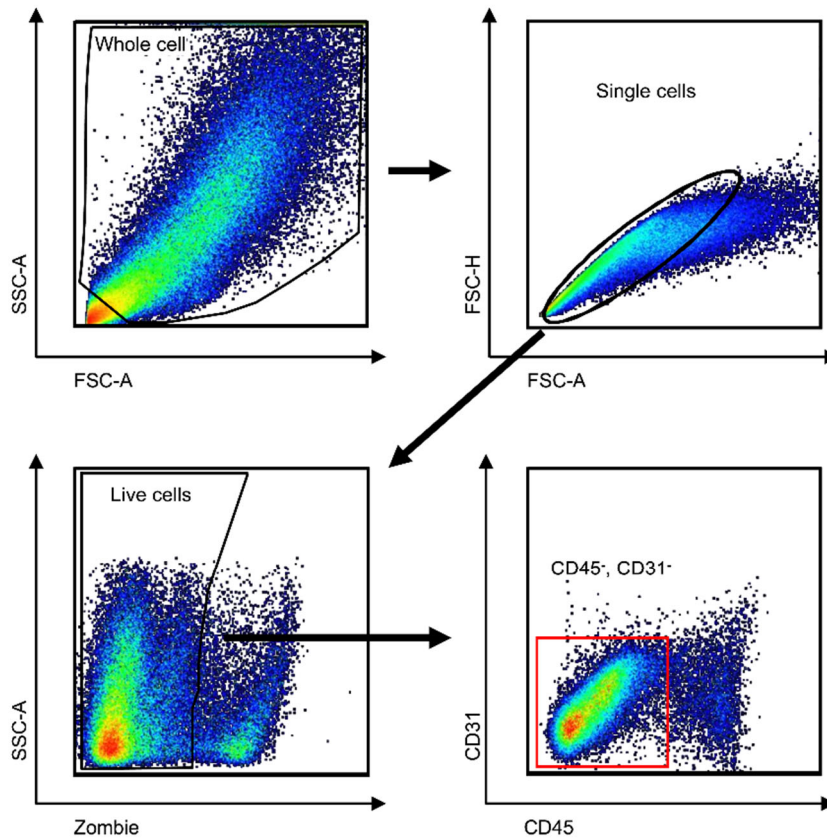
Supplementary Figure S7



Supplementary Figure S7. PD-L1 expression in FEF3 stimulated by TGF- β or conditioned medium of esophageal squamous cell carcinoma cells

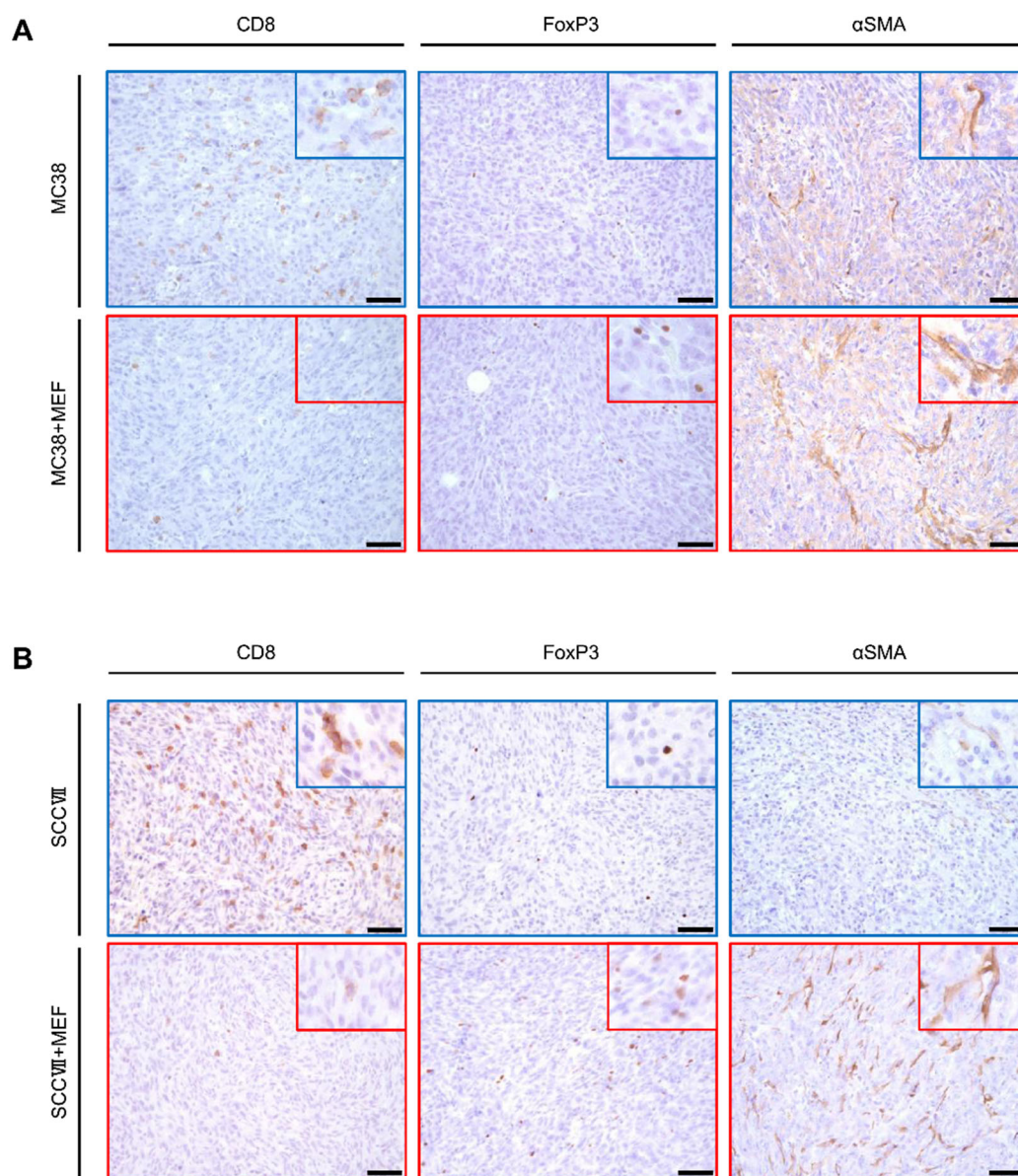
Western blotting was performed as described previously. The following antibodies were used; monoclonal anti-E-cadherin (#3195 clone, 24E10, Cell Signaling Technology), monoclonal anti-vimentin (#5741, clone D21H3, Cell Signaling Technology), monoclonal anti- α SMA (#19245, clone D4K9N, Cell Signaling Technology), polyclonal anti-FAP (ab53066, Abcam), monoclonal anti-PD-L1 (#13684, clone E1L3N, Cell Signaling Technology), and monoclonal anti- β -actin (A5441, clone AC-15, Sigma-Aldrich). The membranes were visualized using an Amersham Imager 600 (GE Healthcare, Little Chalfont/ UK). (A, B) FEF3 activated by (A) TGF- β and (B) conditioned medium of TE4 and TE8 subjected to western blotting of α SMA, FAP, PD-L1, and β -actin expression. (C, D) Flow cytometry analysis of cell surface PD-L1 expression in human cancer cells and fibroblasts in a co-culture model of TE4 and FEF3. (C) Histogram and (D) comparison of PD-L1 expression. (E, F) Flow cytometry analysis of cell surface PD-L1 expression in human cancer cells and fibroblasts in a co-culture model of TE8 and FEF3. (E) Histogram and (F) comparison of PD-L1 expression. n = 3, comparative analysis of mean fluorescence intensities by ratio paired t-test, *P < 0.05.

Supplementary Figure S8



Supplementary Figure S8. Gating strategy and evaluation for PD-L1 in cancer cells and CAFs in vivo models

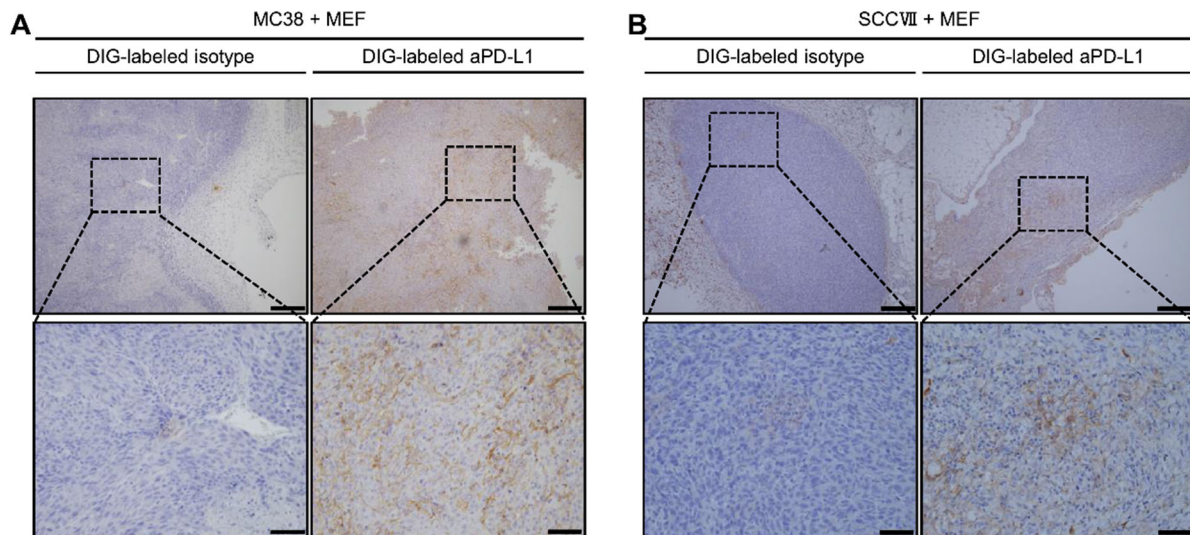
Gating strategy and representative flow cytometry plots. we carried out dead cell removal and subsequently gated out CD45 and CD31. The CD90.2 positive cells were identified as CAFs, while the CD90.2 negative cells were identified as cancer cells.

Supplementary Figure S9

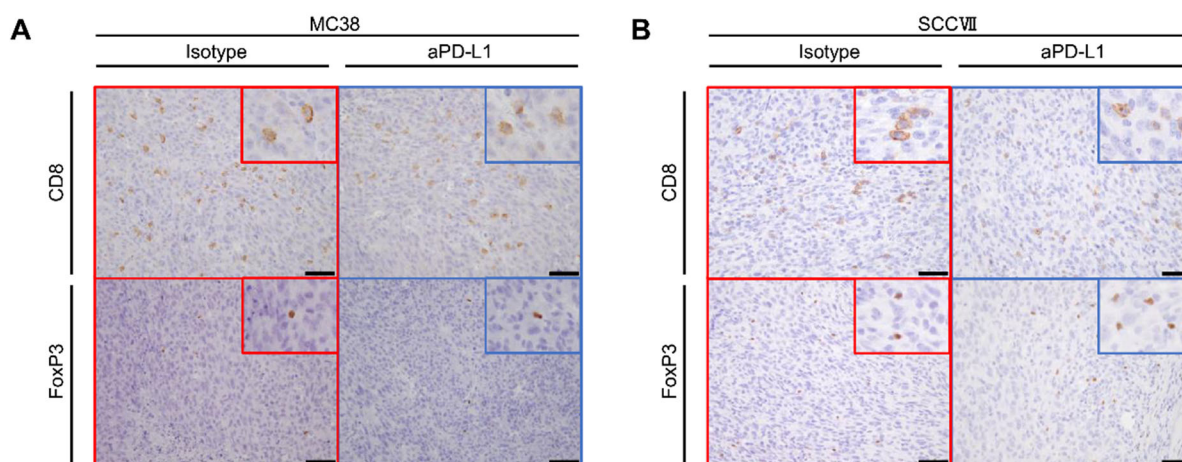
Supplementary Figure S9. Representative pictures of immunohistochemical staining for CD8, FoxP3, and α SMA in tumor tissues

(A) MC38 cells with and without MEF tumors. (B) SCCVII with or without MEF tumors.

Scale bars = 50 μ m.

Supplementary Figure S10**Supplementary Figure S10. Digoxigenin-labeled anti-PD-L1 antibody administration for murine subcutaneous tumors**

(A, B) Representative pictures of immunohistochemical staining for Digoxigenin (DIG)-labeled anti-PD-L1 antibody (aPD-L1) and DIG-labeled isotype rat IgG2b. (A) MC38+MEF. (B) SCCVII+MEF. Scale bars = 200 μm . Lower figures are enlarged images. Scale bars = 50 μm .

Supplementary Figure S11

Supplementary Figure S11. Representative pictures of immunohistochemical staining for CD8 and FoxP3 in MC38 and SCCVII tumors without MEF

(A) MC38 tumor without MEF. (B) SCCVII tumor without MEF. Scale bars = 50 μ m.

Supplementary Table S1. Clinicopathological features for PD-L1 in cancer cells

Variable	Total n = 140	PD-L1(+) n = 60 (42.9%)	PD-L1(-) n = 80 (57.1%)	P value
Age (years)	67 (40–85)	67 (44–85)	67 (40–84)	0.644§
Sex (male/female)				0.626†
Male	121 (86.4%)	53 (88.3%)	68 (85.0%)	
Female	19 (13.6%)	7 (11.7%)	12 (15.0%)	
Neo-adjuvant chemotherapy	35 (25.0%)	18 (30.0%)	17 (21.2%)	0.245†
Tumor location				0.089†
Cervical	12 (8.6%)	4 (6.7%)	8 (10.0%)	
Upper	24 (17.1%)	5 (8.3%)	19 (23.8%)	
Middle	60 (42.9%)	30 (50.0%)	30 (37.5%)	
Lower	28 (20.0%)	15 (25.0%)	13 (16.2%)	
Abdominal	16 (11.4%)	6 (10.0%)	10 (12.5%)	
Pathological T stage				< 0.001*
T1	62 (44.3%)	14 (23.3%)	48 (60.0%)	
T2	15 (10.7%)	7 (11.7%)	8 (10.0%)	
T3	59 (42.1%)	38 (63.3%)	21 (26.2%)	
T4	4 (2.9%)	1 (1.7%)	3 (3.8%)	
Pathological N stage				0.054†
N0	68 (48.6%)	23 (38.3%)	45 (56.2%)	
N1	38 (27.1%)	16 (26.7%)	22 (27.5%)	
N2	21 (15.0%)	12 (20.0%)	9 (11.2%)	
N3	13 (9.3%)	9 (15.0%)	4 (5.0%)	
Histological type				0.422†
Squamous cell carcinoma	123 (87.9%)	55 (91.7%)	68 (85.0%)	
Adenocarcinoma	12 (8.6%)	3 (5.0%)	9 (11.2%)	
Other	5 (3.6%)	2 (3.3%)	3 (3.8%)	
αSMA Area Index	7.76 (0.49–40.30)	12.83 (1.39–33.25)	4.73 (0.49–40.30)	< 0.001§*
FAP Area Index	6.04 (0.01–39.91)	8.54 (0.5–37.0)	3.97 (0.01–39.91)	< 0.001§*
CD8	40.13 (0.25–215.75)	43.38 (0.25–185.25)	38.13 (0.50–215.75)	0.931§
FoxP3	15.13 (0.5–138)	20.75 (2.0–138)	11.86 (0.50–52.5)	0.001§*

Values are presented as median or n (%)

Mann-Whitney *U* test: §, Fisher's exact test: †, * $P < 0.05$ (statistical significance)

SMA, smooth muscle actin; FAP, fibroblast activation protein; FoxP3, forkhead box p3; PD-L1, programmed cell death ligand 1

Supplementary Table S2. Univariate and multivariate analysis for overall survival

Variable	Unfavorable/ favorable	Univariate analysis			Multivariate analysis		
		HR	95% CI	<i>P</i> value	HR	95% CI	<i>P</i> value
Age (years)	≥70/ < 70	1.09	0.67–1.79	0.720			
Sex	Male/Female	2.91	1.06–8.00	0.039*	2.88	1.04–7.97	0.041*
Neoadjuvant chemotherapy	Yes/No	2.20	1.33–3.63	0.002*	1.50	0.88–2.54	0.132
Pathological T stage	T2, T3, T4/T1	2.55	1.51–4.31	< 0.001*	1.46	0.79–2.69	0.226
Pathological N stage	N1, N2, N3/N0	2.71	1.61–4.54	< 0.001*	2.01	1.15–3.55	0.015*
PD-L1 in cancer cells	Positive/Negative	2.22	1.37–3.61	0.001*	1.72	1.03–2.87	0.039*

Cox proportional hazard model, * $P < 0.05$ (statistical significance)

HR, hazard ratio; CI, confidence interval; PD-L1, programmed cell death 1.

Multivariate analysis was performed on statistically significant parameters obtained from the univariate.

Supplementary Table S3. Univariate and multivariate analysis for relapse-free survival

Variable	Unfavorable/favorable	Univariate analysis			Multivariate analysis		
		HR	95% CI	<i>P</i> value	HR	95% CI	<i>P</i> value
Age (years)	≥70/ < 70	0.97	0.60–1.57	0.892			
Sex	Male/Female	3.06	1.11–8.40	0.030*	2.79	1.01–7.74	0.048*
Neoadjuvant chemotherapy	Yes/No	2.76	1.68–4.53	< 0.001*	1.58	0.88–2.81	0.122
Pathological T stage	T2, T3, T4/T1	2.84	1.70–4.76	< 0.001*	2.05	1.21–3.49	0.008*
Pathological N stage	N1, N2, N3/N0	2.72	1.64–4.49	< 0.001*	2.14	1.27–3.60	0.004*
PD-L1 in cancer cells	Positive/Negative	2.41	1.50–3.88	< 0.001*	2.02	1.22–3.34	0.006*

Cox proportional hazard model, **P* < 0.05 (statistical significance)

HR, hazard ratio; CI, confidence interval; PD-L1, programmed cell death 1.

Multivariate analysis was performed on statistically significant parameters obtained from the univariate.

Supplementary Table S4. Univariate and multivariate analysis for PD-L1 expression in cancer cells

Variable	Unfavorable/favorable	Univariate analysis			Multivariate analysis		
		OR	95% CI	<i>P</i> -value	OR	95% CI	<i>P</i> -value
Age (years)	≥70/<70	1.04	0.52–2.07	0.920			
Sex	Male/Female	1.34	0.49–3.63	0.570			
Neo-adjuvant chemotherapy	Yes/No	1.59	0.74–3.43	0.239			
Pathological T stage	T2, T3, T4/T1	4.93	2.34–10.40	< 0.001*	2.29	0.87–6.02	0.093
Pathological N stage	N1, N2, N3/N0	2.07	1.05–4.09	0.037*	0.73	0.30–1.78	0.489
Area index of αSMA	Positive/Negative	1.83	1.08–3.10	0.024*	4.72	1.81–12.30	0.001*

Logistic regression analysis, **P* < 0.05 (statistical significance)

OR, odds ratio; CI, confidence interval; SMA, smooth muscle actin.

Multivariate analysis was performed on statistically significant parameters obtained from the univariate.